

Synthesis, molecular structure, and stability of a zirconocene derivative with α -Keggin mono-aluminum-substituted polyoxotungstate†

Cite this: *Dalton Trans.*, 2013, **42**, 1129Chika Nozaki Kato,^{*a} Yuki Makino,^a Wataru Unno^a and Hidemitsu Uno^b

The synthesis and crystal structure of a zirconocene derivative with α -Keggin mono-aluminum-substituted polyoxotungstate, $[\alpha\text{-PW}_{11}\text{Al}(\text{OH})\text{O}_{39}\text{ZrCp}_2]_2^{6-}$ ($\text{Cp} = \text{C}_5\text{H}_5^-$) (**1**), which was obtained by the reaction of α -Keggin mono-aluminum-substituted polyoxotungstate with a biscyclopentadienylzirconium(IV) complex, is described herein. Analytically pure, homogeneous, yellow crystals of the tetra-*n*-butylammonium salt of polyoxoanion **1**, $[(n\text{-C}_4\text{H}_9)_4\text{N}]_6[\alpha\text{-PW}_{11}\text{Al}(\text{OH})\text{O}_{39}\text{ZrCp}_2]_2$ (**TBA-1**), were obtained from the ca. 1 : 1 reaction of $[(n\text{-C}_4\text{H}_9)_4\text{N}]_4[\alpha\text{-PW}_{11}\{\text{Al}(\text{OH}_2)\text{O}_{39}\}]$ with $\text{Cp}_2\text{Zr}(\text{OTf})_2\cdot\text{THF}$ ($\text{OTf} = \text{O}_3\text{SCF}_3^-$) in acetonitrile solution under an argon atmosphere, followed by precipitation from water and crystallization from acetonitrile. **TBA-1** was characterized based on X-ray structure analysis, elemental analysis, thermogravimetric/differential thermal analysis (TG/DTA), Fourier transform infrared (FTIR), and solution (^{31}P , ^{27}Al , ^{19}F , ^1H , and ^{13}C) nuclear magnetic resonance (NMR) spectroscopy. Single-crystal X-ray structure analysis revealed that the two $\{\text{PW}_{11}\text{AlO}_{40}\}$ units are bridged by two "bent sandwich" $\text{Cp}_2\text{Zr}^{2+}$ fragments with C_2 symmetry. Each zirconium center was bound to a terminal oxygen atom of the aluminum and tungsten sites and an edge-sharing oxygen atom at the Al–O–W linkage. Further, the stability towards water was investigated by NMR (^{31}P , ^1H , and ^{13}C) and FTIR spectroscopy. The η^5 -cyclopentadienylzirconium fragments were not eliminated from the surface of $[\alpha\text{-PW}_{11}\{\text{Al}(\text{OH}_2)\text{O}_{39}\}]^{4-}$ even after 24 h exposure to 50 equiv. of water.

Received 12th September 2012,

Accepted 24th October 2012

DOI: 10.1039/c2dt32107f

www.rsc.org/dalton

Introduction

Polyoxometalates¹ are soluble metal oxide clusters that resemble discrete fragments of the solid metal oxides widely used as supports for transition metal heterogeneous catalysts. Given the difficulties in determining the structures and therefore the operative mechanisms of oxide-supported catalysts, rational improvement of such catalysts is problematic, and the attractiveness of using polyoxoanion-supported, atomically dispersed transition metals as analogs becomes apparent. To date, numerous polyoxoanion-supported compounds have

been synthesized by using complete and intact polyoxometalates² containing d^0 transition metals, *e.g.*, $\text{Nb}_6\text{O}_{19}^{8-}$,³ $\text{Nb}_2\text{W}_4\text{O}_{19}^{4-}$,⁴ $\text{A-}\beta\text{-SiW}_9\text{M}_3\text{O}_{40}^{7-}$ ($\text{M} = \text{Nb}^{\text{V}}, \text{V}^{\text{V}}$),⁵ $\text{B-}\alpha\text{-P}_2\text{W}_{15}\text{M}_3\text{O}_{62}^{9-}$ ($\text{M} = \text{Nb}^{\text{V}}, \text{V}^{\text{V}}$),⁶ $\alpha\text{-PW}_{11}\text{NbO}_{40}^{4-}$,⁷ $\text{CITiW}_5\text{O}_{18}^{3-}$,⁸ and $\text{MW}_5\text{O}_{19}^{3-}$ ($\text{M} = \text{Nb}^{\text{V}}, \text{Ta}^{\text{V}}$),⁹ and some of which have been applied as oxidation catalysts,^{6b,10} precursors in the preparation of nanoclusters,¹¹ and transfer reagents;^{7a} however, the available sites for grafting organic and organometallic fragments that have been constructed in mixed-metal polyoxometalates remain limited. Meanwhile, the organic–inorganic hybrids area has undergone significant expansion during the last 10 years.¹² The organic–inorganic hybrid materials that were obtained *via* non-covalent interactions or strong covalent bonds between organic/organometallic fragments and polyoxometalates have attracted considerable interest with respect to their catalytic and sorption properties and potential applications to optical, photochemical, and electrochemical materials. Thus, the development of the available sites in mixed-metal polyoxometalates for grafting reactions of organic and organometallic fragments still has great potential to further expand polyoxometalate chemistry.

Here, we focused on the mono-aluminum-substituted site in α -Keggin structure as a support, and single crystals of a

^aDepartment of Chemistry, Faculty of Science, Shizuoka University, 836 Ohya, Suruga-ku, Shizuoka 422-8529, Japan. E-mail: sckatou@ipc.shizuoka.ac.jp

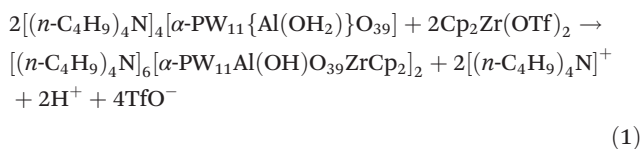
^bDepartment of Chemistry and Biology, Graduate School of Science and Engineering, Ehime University, Matsuyama, 790-8577, Japan

† Electronic supplementary information (ESI) available: Bond lengths and bond angles for **TBA-1** (Table S1); bond valence sum calculations for **TBA-1** (Table S2); ^{19}F NMR spectrum of the product which was obtained by the reaction of $[(n\text{-C}_4\text{H}_9)_4\text{N}]_4[\alpha\text{-PW}_{11}\{\text{Al}(\text{OH}_2)\text{O}_{39}\}]$ with $\text{Cp}_2\text{Zr}(\text{OTf})_2\cdot\text{THF}$ in acetonitrile (Fig. S1); solid-state packing of **TBA-1** (Fig. S2); TG/DTA data of **TBA-1** (Fig. S3); ^1H , ^{13}C , and ^{31}P NMR spectra of the product after a 24 h exposure to water (Fig. S4); FTIR spectrum of the product after a 24 h exposure to water (Fig. S5); ^1H and ^{13}C NMR spectra of $\text{Cp}_2\text{Zr}(\text{OTf})_2\cdot\text{THF}$ (Fig. S6). CCDC 885643. For ESI and crystallographic data in CIF or other electronic format see DOI: 10.1039/c2dt32107f

biscyclopentadienylzirconium(IV) compound with α -Keggin mono-aluminum-substituted phosphotungstate, $[(n\text{-C}_4\text{H}_9)_4\text{N}]_6[\alpha\text{-PW}_{11}\text{Al}(\text{OH})\text{O}_{39}\text{ZrCp}_2]_2$ ($\text{Cp} = \text{C}_5\text{H}_5^-$) (**TBA-1**), suitable for X-ray structure analysis, were successfully obtained. In this study, we report the complete details of the synthesis, molecular structure, and water stability of complex **1**.

Results and discussion

The biscyclopentadienylzirconium(IV) compound with α -Keggin mono-aluminum-substituted phosphotungstate **1** with C_2 symmetry was obtained in 29% yield, based on the tetra-*n*-butylammonium salt $[(n\text{-C}_4\text{H}_9)_4\text{N}]_6[\alpha\text{-PW}_{11}\text{Al}(\text{OH})\text{O}_{39}\text{ZrCp}_2]_2$ (**TBA-1**). Compound **TBA-1** was prepared by the *ca.* 1 : 1 reaction of $[(n\text{-C}_4\text{H}_9)_4\text{N}]_4[\alpha\text{-PW}_{11}\{\text{Al}(\text{OH}_2)\}\text{O}_{39}]$ with $\text{Cp}_2\text{Zr}(\text{OTf})_2\cdot\text{THF}$ in acetonitrile, under an argon atmosphere, followed by precipitation from water in ambient atmosphere. Finally, yellow crystalline products were obtained by crystallization from acetonitrile at 25 °C. The formation of polyoxoanion **1** can be shown by an ionic balance (eqn (1)). The ^{19}F NMR spectrum in CDCl_3 of the product which was obtained by the reaction of $[(n\text{-C}_4\text{H}_9)_4\text{N}]_4[\alpha\text{-PW}_{11}\{\text{Al}(\text{OH}_2)\}\text{O}_{39}]$ with $\text{Cp}_2\text{Zr}(\text{OTf})_2\cdot\text{THF}$ in acetonitrile, followed by evaporation to dryness, showed elimination of TfO^- ($\delta -78.3$) from $\text{Cp}_2\text{Zr}(\text{OTf})_2\cdot\text{THF}$; however, the formation of trifluoromethanesulfonic acid (TfOH) was not observed, as shown in Fig. S1.† $\text{Cp}_2\text{Zr}^{2+}$ fragments were affixed to the surface of the polyoxoanion support, after which treatment with water in air was used to purify the target compound by a precipitation step.



Single crystals of **TBA-1** that were suitable for X-ray crystallography could be obtained by crystallization from acetonitrile *via* slow-evaporation. X-ray structural analysis of crystalline $[(n\text{-C}_4\text{H}_9)_4\text{N}]_6[\alpha\text{-PW}_{11}\text{Al}(\text{OH})\text{O}_{39}\text{ZrCp}_2]_2$ revealed the presence of discrete $[(n\text{-C}_4\text{H}_9)_4\text{N}]^+$ cations and $[\alpha\text{-PW}_{11}\text{Al}(\text{OH})\text{O}_{39}\text{ZrCp}_2]_2^{6-}$ anions, shown in Fig. 1, in which two $\{\text{PW}_{11}\text{AlO}_{40}\}$ units are bridged by two “bent sandwich” $\text{Cp}_2\text{Zr}^{2+}$ fragments with C_2 symmetry. The solid-state packing of **TBA-1** is illustrated in Fig. S2.† Selected bond lengths and angles around the zirconium center in **1** are summarized in Table 1, while other bond lengths (Å) and angles (°) (Table S1†) and the bond valence sum (BVS) calculations of the W, P, Al, and O atoms (Table S2) are given in ESI.† Each zirconium center was bound to the terminal oxygen atoms of the Al and W sites and to the edge-sharing oxygen atom of the Al–O–W linkage with 5-coordination geometry. The bond lengths of the two W–O linkages bound to the zirconium centers, W(1)–O(24) and W(3)–O(22), were 1.754(14) and 1.730(14) Å, respectively. In addition, the bond lengths of the Al–O linkages bound to the zirconium centers (Al(1)–O(26) and Al(2)–O(23)) were 1.858(14) and

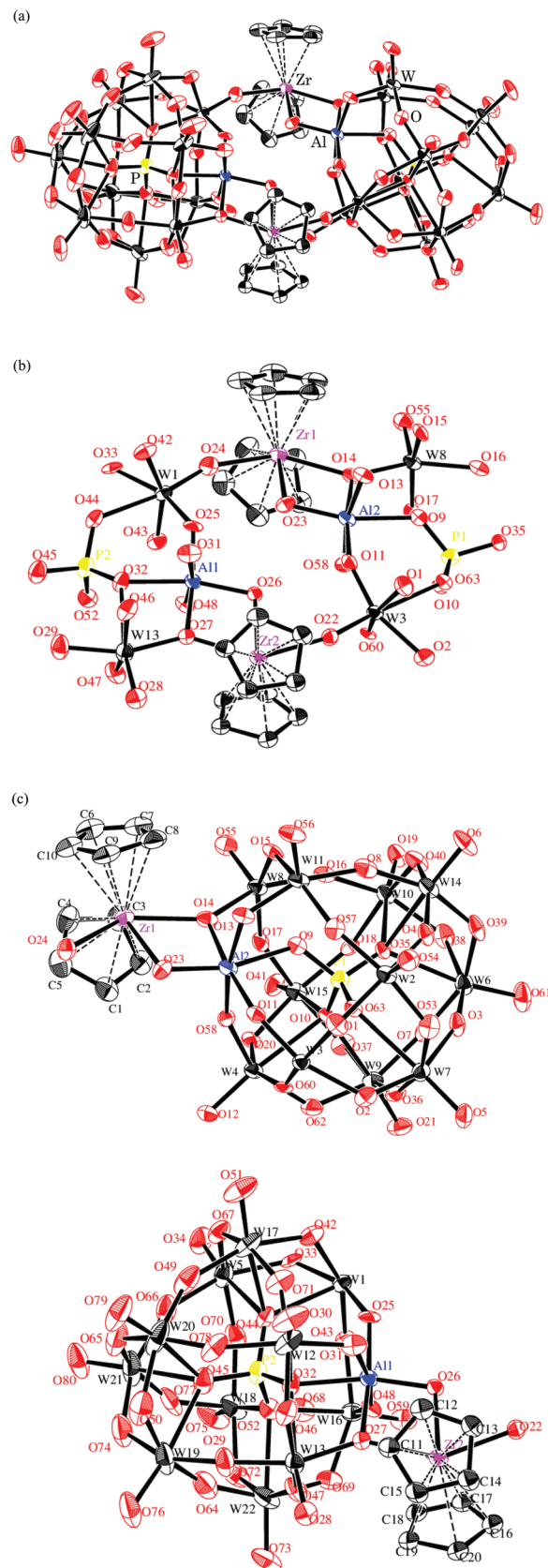
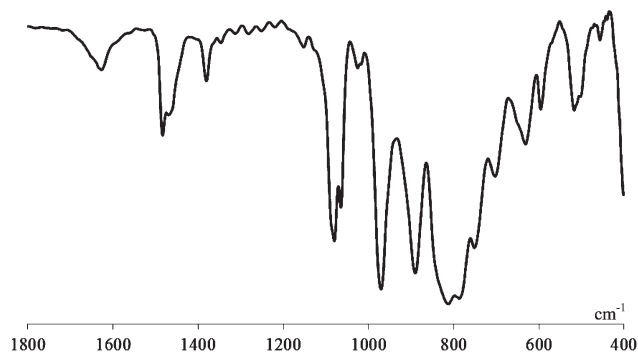


Fig. 1 (a) Molecular structure of the polyoxoanion $[\alpha\text{-PW}_{11}\text{Al}(\text{OH})\text{O}_{39}\text{ZrCp}_2]_2^{6-}$ (**1**), (b) the partial structure around the zirconium and aluminum sites, and (c) the partial structures of Keggin units with atom numberings.

Table 1 Selected bond distances and angles around zirconium and aluminum sites in **1**

Distances (Å)			
Al(1)–O(25)	1.911(15)	W(1)–O(24)	1.754(14)
Al(1)–O(26)	1.858(14)	W(1)–O(25)	1.826(14)
Al(1)–O(27)	1.923(16)	W(1)–O(33)	2.000(14)
Al(1)–O(31)	1.848(16)	W(1)–O(42)	1.958(15)
Al(1)–O(32)	2.117(14)	W(1)–O(43)	1.890(14)
Al(1)–O(48)	1.864(15)	W(1)–O(44)	2.356(14)
Al(2)–O(9)	2.119(14)	W(3)–O(1)	1.934(15)
Al(2)–O(11)	1.899(15)	W(3)–O(2)	2.010(14)
Al(2)–O(13)	1.889(14)	W(3)–O(11)	1.798(14)
Al(2)–O(14)	1.955(15)	W(3)–O(22)	1.730(14)
Al(2)–O(23)	1.848(14)	W(3)–O(60)	1.871(13)
Al(2)–O(58)	1.865(14)	W(3)–O(63)	2.371(13)
Zr(1)–O(14)	2.275(14)	W(8)–O(9)	2.462(14)
Zr(1)–O(23)	2.263(14)	W(8)–O(14)	1.895(14)
Zr(1)–O(24)	2.220(14)	W(8)–O(15)	1.910(14)
Zr(2)–O(22)	2.251(13)	W(8)–O(16)	1.963(14)
Zr(2)–O(26)	2.194(13)	W(8)–O(17)	1.929(13)
Zr(2)–O(27)	2.211(13)	W(8)–O(55)	1.686(15)
P(1)–O(9)	1.527(14)	W(13)–O(27)	1.927(13)
P(2)–O(32)	1.512(15)	W(13)–O(28)	1.689(15)
Zr(1)⋯Zr(2)	7.917(2)	W(13)–O(29)	1.907(15)
Al(1)⋯Al(2)	5.3178(8)	W(13)–O(32)	2.451(14)
Zr(1)–centroid Cp(1–5)	2.222(11)	W(13)–O(46)	1.925(16)
Zr(1)–centroid Cp(6–10)	2.264(11)	W(13)–O(47)	1.873(16)
Zr(2)–centroid Cp(11–15)	2.259(9)		
Zr(1)–centroid Cp(16–20)	2.236(10)		
Angles (°)			
Al(1)–O(26)–Zr(2)	105.4(6)	W(1)–O(24)–Zr(1)	158.9(8)
Al(2)–O(23)–Zr(1)	105.0(7)	W(3)–O(22)–Zr(2)	160.4(8)
Average	105.3	Average	159.7
O(14)–Zr(1)–O(23)	68.9(5)	W(1)–O(25)–Al(1)	143.3(8)
O(26)–Zr(2)–O(27)	69.2(5)	W(3)–O(11)–Al(2)	145.5(8)
Average	69.1	Average	144.5
O(26)–Al(1)–O(27)	82.9(6)	O(24)–W(1)–O(25)	101.4(6)
O(14)–Al(2)–O(23)	84.9(7)	O(11)–W(3)–O(22)	100.8(6)
Average	84.0	Average	101.2
Cp(1–5)–Zr(1)–Cp(6–10)	125.75(9)		
Cp(11–15)–Zr(2)–Cp(16–20)	129.67(9)		
Average	127.7		

1.848(14) Å, respectively. These lengths were markedly longer than those of the tungsten and terminal oxygen linkages (average 1.7 Å); thus, the Al–O and W–O bonds were stretched to facilitate coordination to the zirconium centers. The bond lengths of the six Zr–O linkages were in the range of 2.194(13) to 2.275(14) Å (average 2.2 Å), which were similar to those of $[\text{Zr}(\alpha_2\text{-P}_2\text{W}_{17}\text{O}_{61})_2]^{16-}$ (average 2.2 Å) and $[\text{Zr}(\alpha\text{-PW}_{11}\text{O}_{39})_2]^{10-}$ (average 2.2 Å).¹³ The Zr–centroid Cp distances were in the range of 2.222(11) to 2.264(11) Å (average 2.25 Å), which were similar to those of $[\text{LAlMe}(\mu\text{-O})\text{ZrMeCp}_2]$ (2.254(2) Å) and $[\text{LAlMe}(\mu\text{-O})\text{ZrClCp}_2]$ ($\text{L} = \text{HC}[\text{CMe}(2,6\text{-iPr}_2\text{C}_6\text{H}_3\text{N})_2]$) (2.246(3) Å).¹⁴ The two Al–O–Zr bonds were significantly bent; the bond angles of Al(1)–O(26)–Zr(2) and Al(2)–O(23)–Zr(1) were 105.4(6)° and 105.0(7)°, respectively. The angles of the W–O–Zr linkages in polyoxoanion **1** were also bent; the bond angles of W(1)–O(24)–Zr(1) and W(3)–O(22)–Zr(2) were 158.9(8)° and 160.4(8)°, respectively. For $[(\text{PW}_{11}\text{O}_{39}\text{NbO})_2\text{ZrCp}_2]^{6-}$,^{7a} the angles of two Nb–O–Zr linkages between the two $\{\text{PW}_{11}\text{NbO}_{40}\}$ units were 159(1)° and 148(1)°, which were larger than those of Al–O–Zr linkages of polyoxoanion **1**. The angles between the centroid Cp rings and zirconium centers were 125.75(9)° and

**Fig. 2** FTIR spectrum in the polyoxoanion region (1800–400 cm^{-1}), as acquired from KBr disks of **TBA-1**.

129.67(9)°, which were similar to that of $[(\text{PW}_{11}\text{O}_{39}\text{NbO})_2\text{ZrCp}_2]^{6-}$ (131°).

The values of the bond valence sums (BVSs) for **TBA-1**,¹⁵ which were calculated based on the observed bond lengths, were in the range of 5.664–6.485 (average 5.997) for the 22 W atoms, 4.816–5.125 (4.971) for the two P atoms, 2.673–2.740 (2.707) for two Al atoms, and 1.488–2.075 (1.897) for the 78 O atoms, excluding O(23) and O(26); these values were within reasonable agreement with the formal valences of W^{6+} , P^{5+} , Al^{3+} , and O^{2-} , respectively (Table S2†). The calculated BVS values of O(23) and O(26) at the two Al–O–Zr linkages were 0.9444 and 1.013, respectively, suggesting that a proton was bound to each of the two bridging oxygen atoms between the aluminum and zirconium atoms.

Elemental analysis of **TBA-1** dried overnight at room temperature under 10^{-3} – 10^{-4} Torr of vacuum prior to analysis was consistent with the composition $[(n\text{-C}_4\text{H}_9)_4\text{N}]_6[\alpha\text{-PW}_{11}\text{Al}(\text{OH})\text{O}_{39}\text{ZrCp}_2]_2$. The elemental analysis result also supported the presence of two protons in **TBA-1**. The weight loss observed during the course of drying prior to analysis was 0.30%, suggesting the absence of solvent molecules. This was also supported by the ^1H NMR spectrum, as shown in the Experimental section. A weight loss of 23.0% with an exothermic point at 364 °C was observed within the temperature range from 24.3 to 500 °C in the TG/DTA performed under atmospheric conditions (Fig. S3†); calculations were consistent with the loss of six $[(n\text{-C}_4\text{H}_9)_4\text{N}]^+$ (calcd 19.8%) and four cyclopentadienyl groups (calcd 3.6%) (total: 23.4%).

The FTIR spectrum acquired in the polyoxometalate region of **TBA-1** from a KBr disk of the compound is presented in Fig. 2. The IR spectrum of **TBA-1** (1080, 1065, 1026, 971, 890, 812, 788, 752, 703, and 631 cm^{-1}) was different from that of $[(n\text{-C}_4\text{H}_9)_4\text{N}]_4[\alpha\text{-PW}_{11}\{\text{Al}(\text{OH}_2)\text{O}_{39}\}]$ (1078, 964, 887, 818, 749, and 702 cm^{-1}). In particular, coordination of the $\text{Cp}_2\text{Zr}^{2+}$ fragment is evidenced by a split in the P–O band of $[\alpha\text{-PW}_{11}\{\text{Al}(\text{OH}_2)\text{O}_{39}\}]^{4-}$ at 1078 cm^{-1} into two peaks at 1080 and 1065 cm^{-1} . In addition, a new band appeared at 631 cm^{-1} in the **TBA-1** spectrum, which might be due to the formation of Zr–O linkages. A Zr–O linkage was observed at 590 cm^{-1} in the FTIR spectrum of the alumina–zirconia composite powder.¹⁶ A band assigned to the Cp ligands was clearly observed at

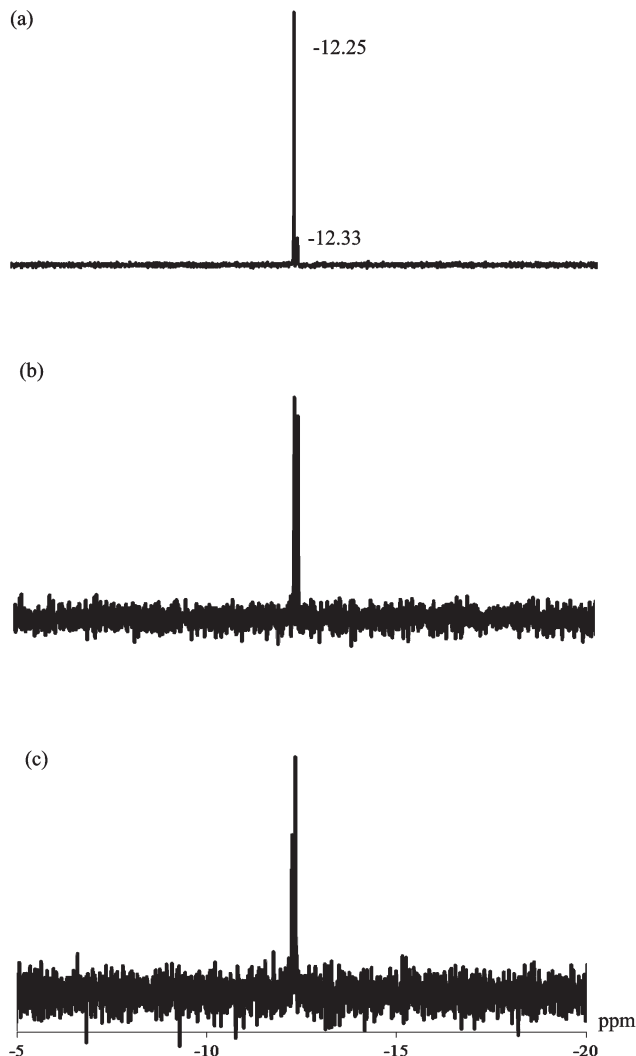


Fig. 3 ^{31}P NMR spectra of (a) as-prepared **TBA-1**, (b) the sample after 12 h exposure to 10 equiv. of water in air, and (c) the sample after 24 h exposure to 50 equiv. of water in air; acquired in CD_3CN .

3120 cm^{-1} . These results suggested that the cyclopentadienyl-zirconium fragments were coordinated to the $[\alpha\text{-PW}_{11}\{\text{Al}(\text{OH}_2)\}\text{O}_{39}]^{4-}$ surface.

Two signals were observed at -12.25 ppm and -12.33 ppm in the ^{31}P NMR spectrum of **TBA-1** acquired in CD_3CN at $25\text{ }^\circ\text{C}$ (Fig. 3(a)). The main signal at -12.25 ppm was assigned to the internal phosphorus atom in polyoxoanion **1**, which was shifted from that of $[(n\text{-C}_4\text{H}_9)_4\text{N}]_4[\alpha\text{-PW}_{11}\{\text{Al}(\text{OH}_2)\}\text{O}_{39}]$ ($\delta -12.48$), whereas the minor signal might be due to a protonated isomer given that the intensity of the signal increased with the addition of 1 equiv. of water, as reported for $[(\text{CH}_3)_2\text{NH}_2]_{10}[\text{Hf}(\text{PW}_{11}\text{O}_{39})_2]\cdot 8\text{H}_2\text{O}$.¹⁷ The ^{27}Al NMR spectrum of **TBA-1** in CD_3CN acquired at $25\text{ }^\circ\text{C}$ was characterized by a broad signal at 17.5 ppm , as shown in Fig. 4. The signal was shifted relative to that of $[(n\text{-C}_4\text{H}_9)_4\text{N}]_4[\alpha\text{-PW}_{11}\{\text{Al}(\text{OH}_2)\}\text{O}_{39}]$ ($\delta 16.1$), suggesting that the cyclopentadienylzirconium fragments were coordinated to the mono-aluminum-substituted sites in **1**. The ^1H NMR spectrum (Fig. 5(a)) of **TBA-1** in CD_3CN

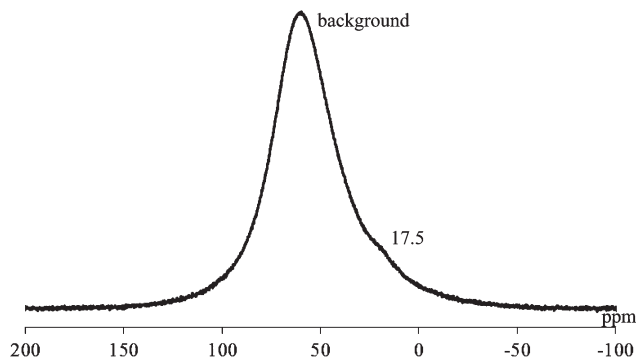


Fig. 4 ^{27}Al NMR spectrum of **TBA-1** in CD_3CN .

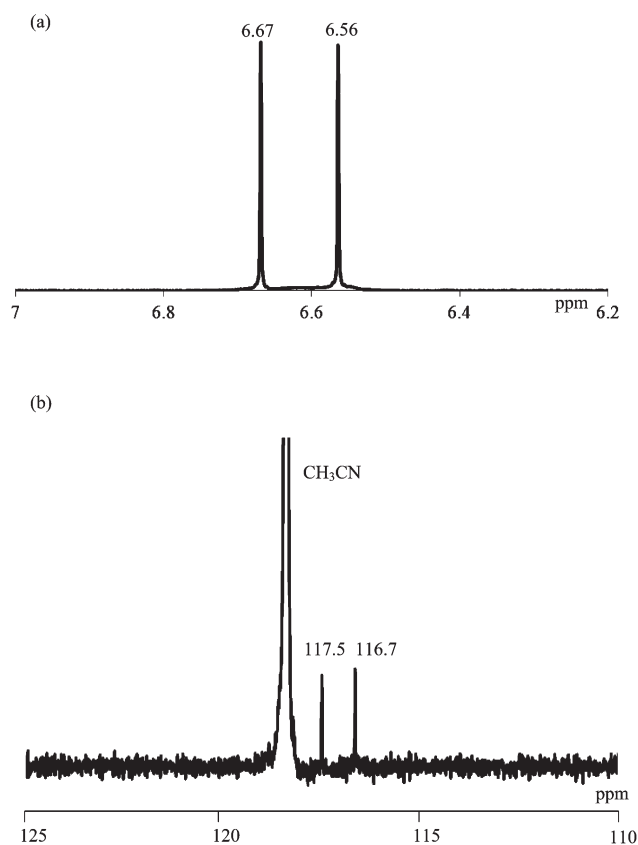


Fig. 5 (a) ^1H NMR and (b) ^{13}C NMR spectra of **TBA-1** in CD_3CN .

at $\sim 25\text{ }^\circ\text{C}$ showed two signals at 6.67 ppm and 6.56 ppm with an intensity ratio of 1 : 1; these peaks were shifted relative to that of $\text{Cp}_2\text{Zr}(\text{OTf})_2\cdot\text{THF}$ ($\delta 6.52$). Two signals were also observed in the ^{13}C NMR spectrum (Fig. 5(b)) at 117.5 ppm and 116.7 ppm with an intensity ratio of 1 : 1; these peaks were shifted from that of $\text{Cp}_2\text{Zr}(\text{OTf})_2\cdot\text{THF}$ ($\delta 117.0$). These two signals are attributed to the two pairs of η^5 -cyclopentadienyl ligands at each zirconium center, shown in the X-ray crystal structure of **1**.

The stability of **TBA-1** towards water was also evaluated using ^{31}P and ^1H NMR spectroscopy. Two signals were observed at -12.25 ppm and -12.34 ppm in the ^{31}P NMR

spectrum of **TBA-1** acquired in CD₃CN at ~25 °C after 12 h exposure to 10 equiv. of water in air (Fig. 3(b)). No signals due to the [α-PW₁₂O₄₀]³⁻ (δ -14.6) and [α-PW₁₁O₃₉]⁷⁻ (δ -12.0) were observed.¹⁸ The ¹H NMR spectrum acquired in CD₃CN at ~25 °C also exhibited two signals at 6.66 and 6.56 ppm, and no signal due to the elimination of Cp₂Zr²⁺ fragments from the polyoxoanion surface was observed. Even after a month, the molecular structure of polyoxoanion **1** was completely retained in acetonitrile solution containing 10 equiv. of water. No decomposition of polyoxoanion **1** was observed after 24 h exposure to 50 equiv. of water based on the ³¹P NMR spectrum acquired in CD₃CN at ~25 °C (Fig. 3(c)). When the polyoxoanion **1** (0.081 g; 0.011 mmol) after 24 h exposure to 50 equiv. of water in acetonitrile (4 mL) was precipitated by the addition of water (50 mL), a white-yellow precipitate was obtained in 0.030 g yield. The NMR {³¹P, ¹H, and ¹³C} spectra in CD₃CN and the FTIR spectrum of the obtained product were the same as those of as-prepared **TBA-1** under the present conditions, as shown in Fig. S4 and S5.† Beer and co-workers reported that [(PW₁₁O₃₉NbO)₂ZrCp₂]⁶⁻ was hydrolyzed in the presence of excess water in acetonitrile to form [PW₁₁NbO₄₀]⁴⁻ and the acid condensation product [(PW₁₁NbO₃₉)₂O]⁶⁻.^{7a} Klemperer and co-workers previously reported that the polyoxoanion {[(η⁵-C₅H₅)₂U]₂(μ-κ²O-TiW₅O₁₉)₂]⁴⁻ was quite stable and was not readily attacked by electrophilic and weakly nucleophilic reagents such as H₂O, CH₃CH₂OH, (CH₃)₂CHNO₂, and CH₃CN; however, <10% decomposition was observed after 2 h exposure to 10 equiv. of water based on ¹H NMR data.^{8a} These results show that the η⁵-cyclopentadienylzirconium fragments of polyoxoanion **1** are significantly stable towards water under the given conditions.

Conclusion

An α-Keggin mono-aluminum-substituted polyoxotungstate zirconocene derivative [α-PW₁₁Al(OH)O₃₉ZrCp₂]₂⁶⁻ was successfully obtained as single crystals of the acetonitrile-soluble tetra-*n*-butylammonium salt [(*n*-C₄H₉)₄N]₆[α-PW₁₁Al(OH)O₃₉ZrCp₂]₂ (**TBA-1**) by reacting Cp₂Zr(OTf)₂·THF with the mono-aluminum-substituted polyoxoanion. **TBA-1** was characterized by X-ray structure analysis, elemental analysis, TG/DTA, FTIR, and solution (³¹P, ²⁷Al, ¹⁹F, ¹H, and ¹³C) NMR spectroscopy. The crystal structure shows that the two {PW₁₁AlO₄₀} units are bridged by two “bent sandwich” Cp₂Zr²⁺ fragments with C₂ symmetry. Each zirconium center is bound to the terminal oxygen atoms of aluminum and tungsten sites, and an edge-sharing oxygen atom of the Al–O–W linkage. Furthermore, the polyoxoanion **1** (dissolved in acetonitrile) exhibited high stability towards water. To the best of our knowledge, the polyoxoanion **1** is the first example of the polyoxoanion-supported organometallic compound prepared by using a mono-aluminum-substituted site constructed in a complete and intact polyoxometalate as an atomic-level support.

Experimental section

Materials

[(*n*-C₄H₉)₄N]₄[α-PW₁₁{Al(OH₂)₃}O₃₉] was synthesized by a previously published method.¹⁸ Cp₂Zr(OTf)₂·THF (OTf = CF₃SO₃⁻) was prepared by a modified literature method as follows.¹⁹ A solution of AgOTf (1.290 g; 5.02 mmol) dissolved in 10 mL of THF was slowly added to a solution of Cp₂ZrCl₂ (0.737 g; 2.52 mmol) dissolved in 15 mL of THF in a dry box filled with argon (>99.9995 vol% purity), and the mixture was stirred for 4 h in the dark. A white precipitate was filtered off through a folded filter paper (Whatman #5), and the filtrate was added to 30 mL of *n*-hexane. At this stage, a white precipitate, AgCl, was obtained in 98% yield based on the formula 2[moles of AgCl]/[moles of Cp₂ZrCl₂] × 100. The reaction mixture was allowed to stand overnight in the dark, after which the supernatant solution was removed *via* decantation, and the white crystalline precipitate was washed with a small amount of *n*-hexane. The product was obtained in 30% yield (0.445 g) based on the formula [moles of Cp₂Zr(OTf)₂·THF]/[moles of Cp₂ZrCl₂] × 100. ¹H NMR (CD₃CN, 23.7 °C, Fig. S6(a)†): δ 6.52 (Cp), 3.65 and 1.80 (THF). ¹³C NMR (CD₃CN, 25.1 °C, Fig. S6(b)†): δ 117.0 (Cp), 26.3 and 68.4 (THF). *n*-Hexane (containing ≤0.001% water) and acetonitrile (containing ≤0.001% water) were used as received from commercial sources.

Instrumentation/analytical procedures

Elemental analysis was carried out by using a Mikroanalytisches Labor Pascher (Remagen, Germany) instrument. The samples were dried overnight at room temperature under 10⁻³–10⁻⁴ Torr vacuum before analysis. Infrared spectra were recorded on a Perkin Elmer Spectrum100 FT-IR spectrometer, in KBr disks, at room temperature. Thermogravimetric (TG) and differential thermal analysis (DTA) data were obtained using a Rigaku Thermo Plus 2 series TG/DTA TG 8120. TG/DTA measurements were performed in air with a temperature increase of 4 °C min⁻¹ between 20 and 500 °C. Solution ¹H (600.17 MHz), ¹³C (150.92 MHz), ³¹P {¹H} (242.95 MHz), and ¹⁹F (564.72 MHz) nuclear magnetic resonance (NMR) spectra were recorded in 5 mm outer diameter tubes on a JEOL ECA-600 NMR spectrometer (Shizuoka University). ¹H and ¹³C NMR spectra were measured in CD₃CN with reference to tetramethylsilane (TMS). Chemical shifts are reported as positive for resonances downfield of TMS (δ 0). The ³¹P NMR spectra were measured in CD₃CN with reference to an external standard of 85% H₃PO₄ in a sealed capillary. Chemical shifts were reported as negative on the δ scale for resonances upfield of H₃PO₄ (δ 0). The ¹⁹F NMR spectra were measured in CDCl₃ with reference to an external standard of [(*n*-C₄H₉)₄N]OTf (δ = -78.27 from CFCl₃).²⁰ Chemical shifts were reported as positive on the δ scale for resonances downfield of AlCl₃ (δ 0). The ²⁷Al NMR (156.36 MHz) spectrum in CD₃CN was recorded on a JEOL ECA-600 NMR spectrometer (Kyushu University) using tubes of 5 mm outer diameter. The ²⁷Al NMR spectrum was referenced to an external standard of the saturated AlCl₃-D₂O

solution (substitution method). Chemical shifts were reported as positive on the δ scale for resonances downfield of AlCl_3 (δ 0).

Preparation

$[(n\text{-C}_4\text{H}_9)_4\text{N}]_6[\alpha\text{-PW}_{11}\text{Al}(\text{OH})\text{O}_{39}\text{ZrCp}_2]_2$ (**TBA-1**). The following manipulations were performed in a drybox filled with argon (>99.9995 vol% purity). A solution of $\text{Cp}_2\text{Zr}(\text{OTf})_2\cdot\text{THF}$ (0.5 g; 0.85 mmol) dissolved in 10 mL of acetonitrile was slowly added to a solution of $[(n\text{-C}_4\text{H}_9)_4\text{N}]_4[\alpha\text{-PW}_{11}\{\text{Al}(\text{OH}_2)\}\text{O}_{39}]$ (3.0 g; 0.81 mmol) dissolved in 10 mL of acetonitrile until the solution became cloudy. After stirring for 4 h at 25 °C, the mixed solution was filtered through a folded filter paper (Whatman #5). At this stage, the filtrate was removed from the drybox, and was combined with water (400 mL) in ambient atmosphere. [Note: ^1H NMR spectra in CD_3CN of the reaction mixture of $[(n\text{-C}_4\text{H}_9)_4\text{N}]_4[\alpha\text{-PW}_{11}\{\text{Al}(\text{OH}_2)\}\text{O}_{39}]$ and $\text{Cp}_2\text{Zr}(\text{OTf})_2\cdot\text{THF}$ in acetonitrile showed three signals at 6.70, 6.65, and 6.57 ppm; however the species observed at 6.70 ppm was completely removed by precipitation from water.] The yellow-white precipitate was collected using a membrane filter (JG 0.2 μm), and washed with a small amount of ethanol. The yield of the crude product was 2.621 g. The obtained product was returned to the drybox and dissolved in 10 mL of acetonitrile; yellow crystals were formed after one week. [Note: **TBA-1** can be crystallized from acetonitrile in air; however, the quality of the crystals degrades gradually upon exposure to moisture.] The yield of the product was 1.74 g (the percentage yield of 29% was calculated on the basis of the following: $[\text{moles of TBA-1}]/[\text{moles of } [(n\text{-C}_4\text{H}_9)_4\text{N}]_4[\alpha\text{-PW}_{11}\{\text{Al}(\text{OH}_2)\}\text{O}_{39}]] \times 100$). Elemental analysis results showed C, 19.02, H, 3.24; Al, 0.73; N, 1.23; P, 0.86; W, 55.2; Zr, 2.46%. Calculations for $[(n\text{-C}_4\text{H}_9)_4\text{N}]_6[\alpha\text{-PW}_{11}\text{Al}(\text{OH})\text{O}_{39}\text{ZrCp}_2]_2 = \text{C}_{116}\text{H}_{238}\text{Al}_2\text{N}_6\text{O}_{80}\text{P}_2\text{W}_{22}\text{Zr}_2$: C, 18.98; H, 3.27; Al, 0.74; N, 1.14; P, 0.84; W, 55.1; Zr, 2.49%. A weight loss of 0.30% was observed during drying overnight at room temperature, under a vacuum of 10^{-3} – 10^{-4} Torr prior to analysis, suggesting the removal of weakly solvated or adsorbed acetonitrile molecules; this was also supported by the absence of any signal due to acetonitrile molecules in the ^1H NMR spectrum of the sample after drying overnight acquired in DMSO-d_6 . TG/DTA performed under atmospheric conditions showed a weight loss of 23.0% with an exothermic point at 364.4 °C (observed below 500 °C); the calculated weight loss of 23.4% was consistent with the loss of four Cp ligands and six tetra-*n*-butylammonium ions. IR (KBr disks) in the 1300–400 cm^{-1} region (polyoxometalate region): 1080(s), 1065(m), 1026(w), 971(s), 890(s), 812(s), 788(s), 752(s), 703(m), and 631(m) cm^{-1} . NMR results gave ^1H NMR (CD_3CN , 24.5 °C): δ 6.67 (singlet) and 6.56 (singlet) (Cp), 3.14 (triplet), 1.64 (multiplet), 1.39 (multiplet), and 0.98 (triplet) ($[(n\text{-C}_4\text{H}_9)_4\text{N}]^+$); ^{13}C NMR (CD_3CN , 24.2 °C): δ 117.49 and 116.65 (Cp), 59.42, 24.48, 20.47, and 14.02 ($[(n\text{-C}_4\text{H}_9)_4\text{N}]^+$); ^{31}P NMR (CD_3CN , 22.8 °C): δ -12.25 (main signal), -12.33 (minor signal); ^{27}Al NMR (CD_3CN , 27.1 °C): δ 17.5.

X-ray crystallography

A yellow prism-shaped crystal of **TBA-1** (0.20 \times 0.10 \times 0.05 mm^3) was mounted on a glass fiber. Data were collected on a Rigaku VariMax instrument with Saturn connected to a multi-layer mirror using monochromated Mo K α radiation ($\lambda = 0.71075$ Å) at 121 ± 1 K. Data were collected and processed using the software CrystalClear for Windows. The structural analysis was performed using the CrystalStructure for Windows software. All structures were solved using SHELXS-97 (direct methods) and refined using SHELXL-97.²¹ For polyoxoanion **1**, 22 tungsten atoms, 2 zirconium atoms, 2 phosphorus atoms, 2 aluminum atoms, and 80 oxygen atoms were clearly identified. Thus, the main features of the molecular structure of the polyoxometalate were clarified. The six tetra-*n*-butylammonium ions were also identified; however, acetonitrile solvent molecules could not be modeled due to disorder of the atoms.²² Accordingly, the residual electron density was removed using the SQUEEZE routine in PLATON.²³

Crystal data for TBA-1. $\text{C}_{116}\text{H}_{238}\text{Al}_2\text{N}_6\text{O}_{80}\text{P}_2\text{W}_{22}\text{Zr}_2$; $M = 7340.20$, orthorhombic, space group $P2_12_12_1$ (#19), $a = 14.8501(10)$, $b = 28.331(2)$, $c = 47.428(3)$ Å, $V = 19953(3)$ Å³, $Z = 4$, $D_c = 2.443$ g cm^{-3} , $\mu(\text{Mo K}\alpha) 128.370$ cm^{-1} . $R_1 = 0.0835$ ($I > 2\sigma(I)$), $wR_2 = 0.1613$ (for all data). GOF = 1.143 (201 629 total reflections, 44 976 unique reflections where $I > 2\sigma(I)$). CCDC reference number 885643 contains the supplementary crystallographic data for this paper.

Acknowledgements

This work was supported by a Grant-in-Aid for Scientific Research on Innovative Areas (No. 21200055) of the Ministry of Education, Culture, Sports, Science and Technology, Japan. This research was partially carried out using equipment at the Center for Instrumental Analysis, Shizuoka University.

Notes and references

- (a) M. T. Pope, *Heteropoly and Isopoly Oxometalates*, Springer-Verlag, Berlin, 1983; (b) M. T. Pope and A. Müller, *Angew. Chem., Int. Ed. Engl.*, 1991, **30**, 34; (c) *Polyoxometalates: From Platonic Solids to Anti-Retroviral Activity*, ed. M. T. Pope and A. Müller, Kluwer Academic Publishers, Dordrecht, The Netherlands, 1994; (d) *Chem. Rev.*, 1998, **98**, 1 (special issue on polyoxometalates; Hill, C. L., guest editor); (e) V. W. Day and W. G. Klemperer, *Science*, 1985, **228**, 533; (f) P. Gouzerh and A. Proust, *Chem. Rev.*, 1998, **98**, 77.
- The definition of complete (plenary)^{1b} polyoxometalates excludes syntheses that involve oxygen-ligand-substitution reactions or the addition of metal fragments into vacancies created by removing $\{\text{MO}\}^{n+}$ units.
- (a) C. M. Flynn, Jr. and G. D. Stucky, *Inorg. Chem.*, 1969, **8**, 178; (b) C. M. Flynn, Jr. and G. D. Stucky, *Inorg. Chem.*,

- 1969, **8**, 332; (c) C. M. Flynn, Jr. and G. D. Stucky, *Inorg. Chem.*, 1969, **8**, 335.
- 4 (a) C. J. Besecker and W. G. Klemperer, *J. Am. Chem. Soc.*, 1980, **102**, 7598; (b) C. J. Besecker, W. G. Klemperer and V. W. Day, *J. Am. Chem. Soc.*, 1982, **104**, 6158; (c) C. J. Besecker, V. W. Day, W. G. Klemperer and M. R. Thompson, *J. Am. Chem. Soc.*, 1984, **106**, 4125; (d) C. J. Besecker, V. W. Day, W. G. Klemperer and M. R. Thompson, *Inorg. Chem.*, 1985, **24**, 44; (e) V. W. Day, T. A. Eberspacher, W. G. Klemperer, R. P. Planalp, P. W. Schiller, A. Yagasaki and B. Zhong, *Inorg. Chem.*, 1993, **32**, 1629; (f) V. W. Day, W. G. Klemperer and D. J. Main, *Inorg. Chem.*, 1990, **29**, 2345; (g) W. G. Klemperer and D. J. Main, *Inorg. Chem.*, 1990, **29**, 2355 and references therein.
- 5 (a) R. G. Finke, B. Rapko and P. J. Domaille, *Organometallics*, 1986, **5**, 175; (b) R. G. Finke, C. A. Green and B. Rapko, *Inorg. Synth.*, 1990, **27**, 128; (c) R. G. Finke, K. Nomiya, C. A. Green and M. W. Droegge, *Inorg. Synth.*, 1992, **29**, 239; (d) R. G. Finke, B. Rapko, R. J. Saxton and P. J. Domaille, *J. Am. Chem. Soc.*, 1986, **108**, 2947; (e) Y. Lin, K. Nomiya and R. G. Finke, *Inorg. Chem.*, 1993, **32**, 6040; (f) B. M. Rapko, M. Pohl and R. G. Finke, *Inorg. Chem.*, 1994, **33**, 3625; (g) R. G. Finke and M. W. Droegge, *J. Am. Chem. Soc.*, 1984, **106**, 7274 and references therein.
- 6 (a) D. K. Lyon and R. G. Finke, *Inorg. Chem.*, 1990, **29**, 1787; (b) D. J. Edlund, R. J. Saxton, D. K. Lyon and R. G. Finke, *Organometallics*, 1988, **7**, 1692; (c) K. Nomiya, N. Mizuno, D. K. Lyon, M. Pohl and R. G. Finke, *Inorg. Synth.*, 1997, **31**, 186; (d) R. G. Finke, D. K. Lyon, K. Nomiya, S. Sur and N. Mizuno, *Inorg. Chem.*, 1990, **29**, 1784; (e) A. Trovarelli and R. G. Finke, *Inorg. Chem.*, 1993, **32**, 6034; (f) M. Pohl and R. G. Finke, *Organometallics*, 1993, **12**, 1453; (g) M. Pohl, Y. Lin, T. J. R. Weakley, K. Nomiya, M. Kaneko, H. Weiner and R. G. Finke, *Inorg. Chem.*, 1995, **34**, 767; (h) M. Pohl, D. K. Lyon, N. Mizuno, K. Nomiya and R. G. Finke, *Inorg. Chem.*, 1995, **34**, 1413; (i) K. Nomiya, C. Nozaki, M. Kaneko, R. G. Finke and M. Pohl, *J. Organomet. Chem.*, 1995, **505**, 23; (j) K. Nomiya, H. Torii, C. N. Kato and Y. Sado, *Chem. Lett.*, 2003, **32**, 664 and references therein.
- 7 (a) E. V. Radkov, V. G. Young, Jr. and R. H. Beer, *J. Am. Chem. Soc.*, 1999, **121**, 8953; (b) E. V. Radkov and R. H. Beer, *Inorg. Chim. Acta*, 2000, **297**, 191.
- 8 (a) V. W. Day, C. W. Earley, W. G. Klemperer and D. J. Maltbie, *J. Am. Chem. Soc.*, 1985, **107**, 8261; (b) W. G. Klemperer and B. Zhong, *Inorg. Chem.*, 1993, **32**, 5821.
- 9 V. W. Day, W. G. Klemperer and D. J. Maltbie, *Organometallics*, 1985, **4**, 104.
- 10 (a) N. Mizuno, H. Weiner and R. G. Finke, *J. Mol. Catal. A: Chem.*, 1996, **114**, 15; (b) H. Weiner, A. Trovarelli and R. G. Finke, *J. Mol. Catal. A: Chem.*, 2003, **191**, 253.
- 11 (a) Y. Lin and R. G. Finke, *Inorg. Chem.*, 1994, **33**, 4891; (b) Y. Lin and R. G. Finke, *J. Am. Chem. Soc.*, 1994, **116**, 8335; (c) S. Özkar and R. G. Finke, *J. Am. Chem. Soc.*, 2002, **124**, 5796; (d) M. A. Watzky, E. E. Finney and R. G. Finke, *J. Am. Chem. Soc.*, 2008, **130**, 11959; (e) B. J. Hornstein and R. G. Finke, *Chem. Mater.*, 2004, **16**, 139; (f) L. S. Ott and R. G. Finke, *J. Nanosci. Nanotechnol.*, 2008, **8**, 1551 and references therein.
- 12 (a) A. Dolbecq, E. Dumas, C. R. Mayer and P. Mialane, *Chem. Rev.*, 2010, **110**, 6009; (b) A. Dolbecq, P. Mialane, F. Sècheresse, B. Keita and L. Nadjo, *Chem. Commun.*, 2012, **48**, 8299; (c) A. Proust, R. Thouvenot and P. Gouzerh, *Chem. Commun.*, 2008, 1837.
- 13 C. N. Kato, A. Shinohara, K. Hayashi and K. Nomiya, *Inorg. Chem.*, 2006, **45**, 8108.
- 14 G. Bai, S. Singh, H. W. Roesky, M. Noltemeyer and H. Schmidt, *J. Am. Chem. Soc.*, 2005, **127**, 3449.
- 15 (a) I. D. Brown and D. Altermatt, *Acta Crystallogr., Sect. B: Struct. Sci.*, 1985, **41**, 244; (b) I. D. Brown and R. D. Shannon, *Acta Crystallogr., Sect. A: Cryst. Phys., Diffraction, Theor. Gen. Crystallogr.*, 1973, **29**, 266; (c) I. D. Brown, *Acta Crystallogr., Sect. B: Struct. Sci.*, 1992, **48**, 553; (d) I. D. Brown, *J. Appl. Crystallogr.*, 1996, **29**, 479.
- 16 J. Chandradass and K. H. Kim, *Met. Mater. Int.*, 2009, **15**, 1039.
- 17 Y. Hou, X. Fang and C. L. Hill, *Chem.-Eur. J.*, 2007, **13**, 9442.
- 18 C. N. Kato, Y. Makino, M. Yamasaki, Y. Kataoka, Y. Kitagawa and M. Okumura, *Advances in Crystallization Processes*, InTech, Croatia, 2012.
- 19 S. J. Angus-Dunne, L. E. P. Lee Chin, R. C. Burns and G. A. Lawrence, *Transition Met. Chem.*, 2006, **31**, 268.
- 20 R. A. T. M. Abbenhuis, I. del Río, M. M. Bergshoef, J. Boersma, N. Veldman, A. L. Spek and G. van Koten, *Inorg. Chem.*, 1998, **37**, 1749.
- 21 G. M. Sheldrick, *Acta Crystallogr., Sect. A: Found. Crystallogr.*, 2008, **46**, 112.
- 22 Some acetonitrile molecules were observed in a single crystal of **TBA-1**; however, no acetonitrile solvent molecules were observed by elemental analysis and ¹H NMR spectroscopy. Thus, the solvent molecules evaporate gradually when crystals are removed from acetonitrile solution.
- 23 A. L. Spek, *Acta Crystallogr., Sect. D: Biol. Crystallogr.*, 2009, **65**, 148.